Anomalous Giant Piezoresistance in AlAs 2D Electron Systems with Antidot Lattices

O. Gunawan, T. Gokmen, Y. P. Shkolnikov, E. P. De Poortere, and M. Shayegan

Department of Electrical Engineering, Princeton University, Princeton, New Jersey 08544, USA

(Received 2 July 2007; revised manuscript received 4 October 2007; published 24 January 2008)

An AlAs two-dimensional electron system patterned with an antidot lattice exhibits a giant piezoresistance effect at low temperatures, with a sign opposite to the piezoresistance observed in the unpatterned region. We suggest that the origin of this anomalous giant piezoresistance is the nonuniform strain in the antidot lattice and the exclusion of electrons occupying the two conduction-band valleys from different regions of the sample. This is analogous to the well-known giant magnetoresistance effect, with valley playing the role of spin and strain the role of magnetic field.

DOI: 10.1103/PhysRevLett.100.036602 PACS numbers: 72.20.Fr, 73.23.Ad, 73.63.Hs, 75.47.Jn

Currently there is considerable interest in electronic devices whose operating principles go beyond the conventional, charge-based electronics. A prime example is the giant magnetoresistance (GMR) device [1], one of the first members of a new class of "spintronic" devices [2,3] whose operation rests on the manipulation of electron's spin degree of freedom. In certain solids the electrons can reside in multiple conduction-band minima (or valleys) and therefore have yet another, *valley*, degree of freedom. Here we report a giant, low-temperature piezoresistance (GPR) effect in a two-valley AlAs two-dimensional electron system (2DES) patterned with antidot lattices. The effect is among the strongest seen in any system and allows the detection of minute strains and displacements via a simple resistance measurement. And yet it is anomalous as it has the opposite sign compared to the conventional piezoresistance found in multivalley semiconductors [4,5]. While we do not have a full explanation for the observed GPR effect, we suggest that it is caused by the nonuniform strain and the exclusion of electrons occupying the two conduction-band valleys from different regions of the sample. This is analogous to the operating principle of the GMR effect: here valley plays the role of spin and strain the role of magnetic field. These results highlight the fundamental analogy between the spin and valley degrees of freedom [6,7] and point to new opportunities in developing novel "valleytronic" devices whose functionality relies on the control and manipulation of the electron's valley degree of freedom [8,9].

We performed experiments on a 2DES in a modulation doped, 11-nm-wide AlAs quantum well. In this system the electrons occupy two in-plane, anisotropic conduction-band valleys with elliptical Fermi contours [10], characterized by a heavy longitudinal mass $m_l = 1.1m_0$ and light transverse mass $m_t = 0.2m_0$, where m_0 is electron mass in vacuum. We label these as X and Y valleys, according to the direction of their major axes, [100] and [010], as shown in the lower inset of Fig. 1 [10]. We patterned a Hall bar along the [100] direction using standard photo lithography technique. Then, via electron beam lithography and dry etching using an electron cyclotron resonance etcher we defined three antidot (AD) lattices with periods $a = 1$, 0.8, and 0.6 μm in three regions of the Hall bar, and we left a fourth region unpatterned (blank) (see the upper insets of Fig. 1). Each AD lattice is an array of holes (ADs) etched to a depth of $\simeq$300 nm into the sample thus depleting the 2DES in the hole area (the 2DES is at a depth of $\simeq$100 nm

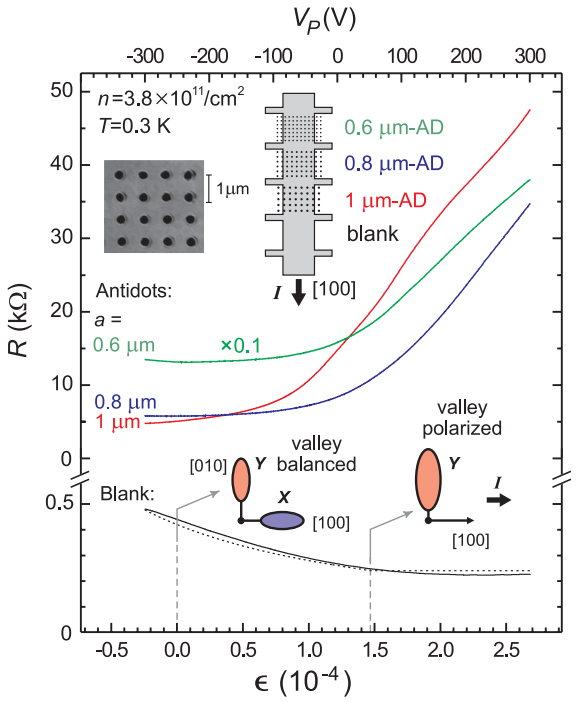

FIG. 1 (color online). The piezoresistance of an AlAs 2DES in the unpatterned (blank) region (lower trace) and in three antidot (AD) regions (upper three traces). The dotted line is the best fit to the piezoresistance in the blank region based on a conventional model. Upper insets: a micrograph of an AD lattice ($a = 0.8$ μm) and sections of the Hall bar. Lower insets: the orientation and occupation of the valleys are schematically shown for the blank region at $\epsilon = 0$ where the two valleys are equally occupied and for $\epsilon > 1.5 \times 10^{-4}$ where all the electrons are transferred to the Y valley.

from the top surface). The ratio d/a for each AD cell is $\sim$1:3, where d is the AD diameter. We also deposited Ti/Au back and front gates to control the total 2DES density (n) in the sample. To apply tunable strain, we glued the sample to one side of a piezo-actuator [10] and monitored the applied strain using a metal-foil strain gauge glued to the piezo's other side. We define strain as $\epsilon = \epsilon_{[100]} - \epsilon_{[010]}$, where $\epsilon_{[100]}$ and $\epsilon_{[010]}$ are the fractional length changes of the sample along the [100] and [010] directions, respectively. Note that for $\epsilon > 0$ electrons are transferred from the X valley to the Y valley while n stays constant [10]. Further fabrication details and characteristics of the blank region of the particular sample used in this study were reported in Ref. [6]. In particular, at a piezo bias (V_P) of -250 V, the X and Y valleys in the blank region are equally occupied (balanced) and, at $n = 3.8 \times 10^{11}/\mathrm{cm}^2$ where the data of Fig. 1 were taken, electrons are all transferred to the Y valley for $V_P > 50$ V ($\epsilon > 1.5 \times 10^{-4}$); see the lower insets in Fig. 1. The measurements were performed in a ^{3}He cryostat with a base temperature of 0.3 K.

The lower trace in Fig. 1 shows the piezoresistance (PR) in the blank region. The PR exhibits the anticipated behavior: the resistance drops with increasing strain as the electrons are transferred to the Y valley whose mobility is higher (because of its smaller effective mass, m_t) along the current direction. Beyond the valley depopulation point ($\epsilon > 1.5 \times 10^{-4}$), the resistance starts to saturate at a low value as the intervalley electron transfer ceases. This is the conventional PR effect in AlAs 2DES as has been reported in Ref. [5]. The dotted line in Fig. 1 represents the best fit of the data to a simple model [5], which assumes that the valley populations change linearly with strain, and adds the conductivities of the two valleys to find the total conductivity; the model also assumes an isotropic scattering time for both valleys and ignores the intervalley scattering.

The upper three traces in Fig. 1 represent the PR of the AD regions and demonstrate our main finding. These traces exhibit an *increasing* resistance as a function of strain, opposite to the PR in the blank region. The strength of the PR effect is also quite prominent in the AD regions: indeed, in the 1-μm-AD region the resistance changes by about 10 times for the range of applied strain while, in contrast, the change for the blank region is only about a factor of 2. Furthermore, for all three AD regions, the PR persists beyond the valley depopulation point of the blank region ($\epsilon > 1.5 \times 10^{-4}$) where the blank region's PR nearly saturates.

These observations highlight the remarkable difference between the PR effect in the blank and the AD regions. We suggest that it is the nonuniform strain distribution in the AD lattice that leads to the anomalous PR. To understand the strain distribution in the AD regions we performed a simple finite-element-method simulation (using FEMLAB) for a plane-strain problem of a 2D medium perforated with an array of holes. We apply a small tensile stress σ_x to the left and right sides, producing a small amount of strain ϵ_0 at $(x, y) \rightarrow \pm\infty$; in other words, if there were no AD lattice, the strain would be uniform everywhere with a magnitude equal to ϵ_0. The result of this simulation is shown in Fig. 2. There is clearly a nonuniform strain distribution due to the presence of the AD lattice. In particular, there are localized regions of enhanced strain (boxes A and B in Fig. 2), and of essentially zero strain (box C). For example, in the upper and lower periphery of the AD (box A) the strain is enhanced by as much as $3\epsilon_0$. This enhancement by $3\epsilon_0$ is indeed indicated by an analytical solution of a 2D plane-strain problem with a single hole [11]. We add that our simulation of Fig. 2 is for a 2D system, however, we expect that in a system which contains an AD lattice at its top surface, the strain profile is qualitatively similar to what is shown in Fig. 2.

But how does a nonuniform strain distribution lead to an increase in resistance? Note that, in our experiment, positive (negative) strain leads to a valley splitting that favors the Y valley (X valley) occupation. This means that, besides being excluded from the AD hole regions, electrons occupying either the X or Y valley feel an extra, modulated, and confining potential as they move through the AD lattice. We suggest that it is this potential that profoundly affects the quasiballistic motion of electrons in the AD region and leads to the observed PR. For example, consider the localized enhancement of positive strain in box A of Fig. 2. Such strain depletes the X-valley electrons in box A and effectively narrows the width of the channels (between the holes) through which they have to travel to carry current. The Y-valley electrons, on the other hand, gradually become the system's majority carriers as strain is increased. But they, too, experience a strongly modulated potential as they travel through the AD lattice (e.g., consider the strain in boxes B, C, and D in Fig. 2). It is likely that such a potential limits the conductivity of the Y-valley electrons. An increase of resistance with the increase of potential modulation amplitude is indeed common in commensurability oscillation experiments on surface grating devices [12]. It is conceivable then, that although Y-valley

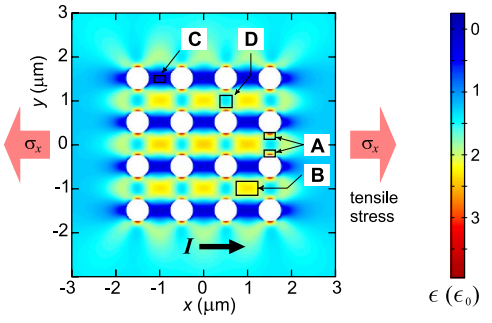

FIG. 2 (color online). Finite element simulation of the strain distribution in a 2D medium perforated with an AD lattice. Boxes A and B highlight areas of enhanced strain while box C marks a region of reduced strain. Strain in box D is close to its average value (ϵ_0).

electrons are favored at high strains, their contribution to the AD lattice conductivity is reduced by the strongly modulated potential.

The above "exclusion" of the different type (X and Y valley) electrons from different regions of the sample suggests a resemblance between our GPR effect and the GMR effect, observed in thin-film structures composed of alternating layers of ferromagnetic and nonmagnetic materials [2,13]. In GMR devices, the reversal of polarization of the magnetization (spin) in the region adjacent to the active channel due to an external magnetic field leads to a narrower effective conducting channel width and additional scattering at the boundaries, both of which lead to higher resistance. We suggest that our GPR effect is analogous to the GMR effect, with valley polarization playing the role of spin polarization and strain the role of magnetic field.

Our magnetoresistance (MR) measurements performed on these AD lattices provide additional clues, as well as interesting puzzles, regarding transport in our samples. In Fig. 3(a) we show resistance (R) versus perpendicular magnetic field (B) traces for the 1 μm-period AD lattice as a function of applied strain (piezo bias); data for the other AD regions are qualitatively similar. At $V_P = -280$ V where, based on the data for the blank region, we expect minimal strain [14], the MR trace exhibits a peak at a field $B_{P,1} = 0.37$ T. We associate this peak with the geometric resonance, or the commensurability [15], of the cyclotron orbit $X1$, shown in the inset to Fig. 3(a). The position of this peak is plotted in Fig. 3(e) versus the reciprocal AD lattice spacing $1/a$. The observed linear dependence is consistent with the expected geometric scaling of the peak position with $1/a$ [16]. In fact, in Ref. [16], systematic measurements and analysis of $B_{P,1}$ as a function of n and a were made in an AlAs 2DES with AD lattices but without any applied strain. Both experimental data and simulations showed that, while the two valleys X and Y could in principle give rise to two sets of commensurate orbits, it is the $X1$ orbit [Fig. 3(a) inset] that gives rise to the fundamental MR peak for current along the [100] direction.

Figure 3(a) reveals that additional MR peaks, which we label with indices $i = 2, 3, \ldots$, and refer to as subharmonic peaks, appear as we strain the AD lattice. These peaks are also observed in MR traces of the other AD lattice regions [Fig. 3(d)], and their positions, $B_{P,i}$, scale linearly with i [Fig. 3(f)]. Such peaks are *not* observed in the absence of strain, e.g., in the experiments of Ref. [16], and their emergence with strain could provide clues for the shape of the potential seen by the X-valley electrons. While subharmonic peaks are seldom seen in AD lattices [17], they are readily observed in transverse magnetic focusing (TMF) experiments [18,19] where ballistic electrons are emitted through a narrow opening and are collected at a second narrow opening which is at a relatively large distance away. Under such conditions, the injected ballistic electrons can bounce off the TMF barrier one or more times as they follow their cyclotron orbit trajectories, and MR peaks are observed whenever the emitter-collector distance equals a multiple integer of the orbit diameter [an illustration of this is shown in Fig. 3(c) for our structure]. We emphasize that in TMF structures, the distance between the emitter and collector is typically larger than the width of the emitter and collector openings thus allowing bouncing trajectories to occur. Furthermore, the narrow openings also produce better focusing and therefore sharp subharmonic peaks.

We hypothesize that the subharmonic peaks observed in Fig. 3 data arise from an effective narrowing of the "emitter and collector openings" and an elongation of the effec-

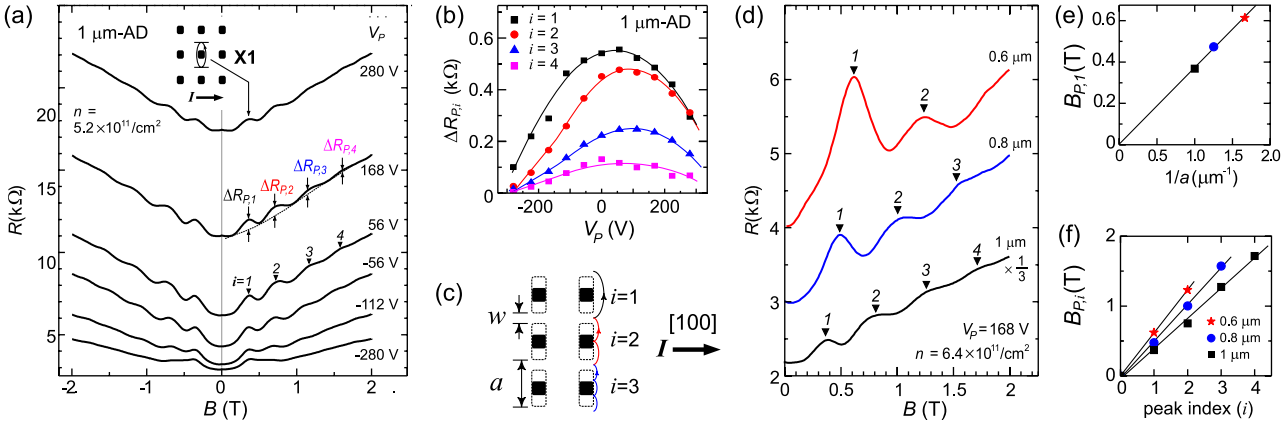

FIG. 3 (color online). (a) Magnetoresistance (MR) traces of the 1 μm-AD region at different values of applied strain, showing the commensurability peaks labeled with indices $i = 1, 2, \ldots$, and the peak amplitudes ($\Delta R_{P,i}$). Inset: $X1$ orbit associated with the fundamental ($i = 1$) peak. (b) Plots of $\Delta R_{P,i}$ as a function of strain. (c) Schematic diagram of the elongated AD lattice with channel width w and period a, and the bouncing orbits that could give rise to subharmonic peaks. The black areas are the original AD (holes); the dotted lines mark the boundaries of the hypothesized, local strain-induced, "extended AD". (d) MR traces of the three AD regions. The MR peak positions in these traces are analyzed in: (e) the $i = 1$ peak position $B_{P,1}$ versus reciprocal AD lattice spacing $1/a$, and (f) peak positions $B_{P,i}$ versus index i. Each set of data points fits well to a straight line that goes through the origin.

tive AD boundary for the X-valley electrons upon the application of strain, as shown in Fig. 3(c). This is suggested by the simulations of Fig. 2 where the X-valley electrons are excluded near the lower and upper boundaries of the ADs (box A) because of the larger local strain. Several features of Fig. 3 data support this hypothesis. (1) As shown in Figs. 3(e) and 3(f) all the peak positions are consistent with the orbit diameters being proportional to a/i. (2) The subharmonic peaks are pronounced only when strain is applied: their amplitudes are indeed small near zero strain, increase with strain, and then decrease at large strain values [Fig. 3(b)]; such behavior is expected since the X-valley electrons should be gradually excluded from the AD lattices (except for the regions marked as box C in Fig. 2). (3) The AD region with the largest period (i.e., the 1 μm-AD) has the most subharmonic peaks; this is consistent with the longer AD boundary allowing more bounces in the electron trajectories. (4) We performed numerical simulations similar to those used in Ref. [16] but with a variable channel width, w, to simulate the strain-induced channel-pinching effect as suggested by Fig. 2 [see Fig. 3(c) for the definition of w]. The results are consistent with our hypothesis: at sufficiently small w indeed a subharmonic peak ($i = 2$) appears and grows in amplitude relative to the fundamental peak as w is made smaller [20,21].

We wish to emphasize that, although the above features of the MR data appear to be consistent with our hypothesis, there are several major puzzles. For example, the density of the X-valley electrons in the ''injection'' channels between the ADs (box D in Fig. 2) is expected to decrease with applied strain and eventually vanish. This implies that the positions of the MR peaks in Fig. 3(a) should shift to smaller B as strain is applied. While we do indeed observe a slight downshift of the peak positions, the amount of the shift is too small considering the magnitude of the applied strain. In fact, the presence of MR peaks [Fig. 3(d)] originating from the X-valley orbits at $V_P = 168$ V ($\epsilon = 2 \times 10^{-4}$) is surprising; if the average strain in the AD lattice regions were the same as in the blank region [14] and the simulation of Fig. 2 were quantitatively accurate, together they would imply that the X-valley electrons should be completely depleted in the channel regions at such strain. More generally, the modulation potential induced by the combination of strain and the AD lattice could considerably modify the band structure and thus the X- and Y-valley splitting. It is not obvious how the commensurate orbits would evolve with strain. We remark, however, that our observation of the subharmonic MR peaks and their evolution with strain are by themselves quite intriguing and, we hope, will stimulate future work [22].

Regardless of its origin, the GPR exhibited by our AD lattices reveals the extreme sensitivity of their resistance to strain. The data of the 1 μm AD lattice, e.g., yield a maximum strain-gauge factor, κ, defined as the fractional change in sample resistance divided by the fractional change in sample length, of over 20 000. This is by far larger than $\kappa \simeq 2$ of standard, metal-foil gauges, and is among the largest κ reported for any solid state material. Our structure may find use as an extremely sensitive, low-temperature PR strain sensor to detect ultrasmall forces and distances. Using a simple resistance measurement, we were able to detect strains down to 10^{-8} with our samples [21]. Given that the spacing between our Hall bar resistance contacts is 40 μm, this strain translates to a displacement of 4×10^{-4} nm (about 1/100 of the Bohr radius). This sensitivity could be further improved by designing AD lattices with optimized shapes and sizes, and using more sophisticated techniques to measure resistance changes.

We thank the ARO and NSF for support, and K. Vakili and J. Shabani for illuminating discussions.

[1] M. N. Baibich *et al.*, Phys. Rev. Lett. **61**, 2472 (1988).
[2] G. A. Prinz, Science **282**, 1660 (1998).
[3] S. A. Wolf *et al.*, Science **294**, 1488 (2001).
[4] C. S. Smith, Phys. Rev. **94**, 42 (1954).
[5] Y. P. Shkolnikov *et al.*, Appl. Phys. Lett. **85**, 3766 (2004).
[6] O. Gunawan *et al.*, Phys. Rev. Lett. **97**, 186404 (2006).
[7] O. Gunawan *et al.*, Nature Phys. **3**, 388 (2007).
[8] O. Gunawan *et al.*, Phys. Rev. B **74**, 155436 (2006).
[9] A. Rycerz *et al.*, Nature Phys. **3**, 172 (2007).
[10] M. Shayegan *et al.*, Phys. Status Solidi B **243**, 3629 (2006).
[11] See, e.g., D. Roylance, *Mechanics of Materials* (Wiley, New York, 1995), p. 186.
[12] P. H. Beton *et al.*, Phys. Rev. B **42**, 9229 (1990).
[13] W. F. Egelhoff *et al.*, J. Vac. Sci. Technol. B **17**, 1702 (1999); also, see Fig. 3 of Ref. [2].
[14] The strain in the AD lattice regions could be somewhat different from the blank region.
[15] D. Weiss *et al.*, Phys. Rev. Lett. **66**, 2790 (1991).
[16] O. Gunawan *et al.*, Phys. Rev. B **75**, 081304(R) (2007).
[17] E. B. Olshanetsky *et al.*, Europhys. Lett. **76**, 657 (2006).
[18] H. van Houten *et al.*, Phys. Rev. B **39**, 8556 (1989).
[19] F. Nihey *et al.*, Appl. Phys. Lett. **57**, 1218 (1990).
[20] Note also that, as might be expected (for transport by X-valley electrons only), the simulations show an overall increase in resistance at $B = 0$ for narrower w, consistent with the PR data of Fig. 1.
[21] O. Gunawan, Ph.D. thesis, Princeton University, 2007.
[22] An alternative explanation for the subharmonic MR peaks could be the ''rosette-shaped'' skipping orbits that go around the ADs and can give rise to MR maxima; see, e.g., Ref. [17]. Yet another possibility could be that the X-valley electrons get trapped in the regions where strain is minimum (box C in Fig. 2), and execute skipping orbits inside these regions.